Stem Cell Reports
Article

OPEN ACCESS

Long-Term Engraftment of ESC-Derived B-1 Progenitor Cells Supports HSC-Independent Lymphopoiesis

Yang Lin,[1] Michihiro Kobayashi,[3] Nathalia Azevedo Portilho,[3] Akansha Mishra,[1] Hongyu Gao,[2] Yunlong Liu,[2] Pamela Wenzel,[3] Brian Davis,[3] Mervin C. Yoder,[1] and Momoko Yoshimoto[3,*]

[1]Department of Pediatrics, Wells Center for Pediatric Research, Indiana University School of Medicine, Indianapolis, IN 46202, USA
[2]Department of Medical and Molecular Genetics, Indiana University School of Medicine, Indianapolis, IN 46202, USA
[3]Center for Stem Cell Research, Institute of Molecular Medicine, McGovern Medical School, University of Texas Health Science Center at Houston, Houston, TX 77030, USA
*Correspondence: momoko.yoshimoto@uth.tmc.edu
https://doi.org/10.1016/j.stemcr.2019.01.006

SUMMARY

It is generally considered that mouse embryonic stem cell (ESC) differentiation into blood cells *in vitro* recapitulates yolk sac (YS) hematopoiesis. As such, similar to YS-derived B-progenitors, we demonstrate here that ESC-derived B-progenitors differentiate into B-1 and marginal zone B cells, but not B-2 cells in immunodeficient mice after transplantation. ESC-derived B-1 cells were maintained in the recipients for more than 6 months, secreting natural IgM antibodies *in vivo*. Gene expression profiling displayed a close relationship between ESC- and YS-derived B-1 progenitors. Because there are no hematopoietic stem cells (HSCs) detectable in our ESC differentiation culture, successful long-term engraftment of ESC-derived functional B-1 cells supports the presence of HSC-independent B-1 cell development.

INTRODUCTION

Hematopoietic stem cells (HSCs) in the adult bone marrow (BM) provide all types of blood cells throughout life, while also self-renewing to maintain blood homeostasis. Blood/marrow stem cell transplantation is the most advanced method to cure patients suffering from hematological malignancies and hematopoietic diseases. Consequently, tremendous effort has been dedicated to establishing a system to produce HSCs from pluripotent stem cells (PSCs) such as embryonic stem cells (ESCs) or inducible PSCs. Overexpressing the *Hoxb4* gene (Kyba et al., 2002; Wang et al., 2005), teratoma formation *in vivo* (Amabile et al., 2013; Suzuki et al., 2013; Tsukada et al., 2017), and direct reprogramming by introducing multiple transcriptional factors into endothelial cells (ECs) (Sugimura et al., 2017) have demonstrated successful engraftment of PSC-derived hematopoietic cells. Similarly, a recent advance has reported that *Hoxb4* expression combined with Delta-like 1 signaling enables mouse ESC-derived hematopoietic progenitor cells (HPCs) to engraft immunodeficient mice with a functional adaptive immune system (Lu et al., 2016). While these PSC-derived functional HSCs have been reported, low chimerism remains a persistent problem and it is still challenging to produce an HSC *in vitro* with equivalent properties of *in vivo* HSCs without gene manipulation. Although conventional ESC differentiation by embryoid body formation or OP9 co-culture produces erythromyeloid, B and T lymphoid cells, no transplantable HSCs are produced (Nakano et al., 1994; Schmitt et al., 2004; Yoshimoto et al., 2009). In this sense, conventional ESC differentiation reflects HSC-independent hematopoiesis and mimics yolk sac (YS) hematopoiesis before HSC emergence at the later stage (Irion et al., 2010; Lin et al., 2014; Yoshimoto, 2015).

There are several waves of hematopoiesis in the YS before the detection of the first HSCs at embryonic day 11.5 (E11.5) in the aorta-gonado-mesonephros region that repopulate lethally irradiated adult mice (Hadland and Yoshimoto, 2017; Lin et al., 2014). These waves include primitive erythroid cells and primitive macrophages at around E7.5 in the YS and definitive (adult) type erythromyeloid progenitors from E8.5 to E9.5 YS. These waves have been considered transient, diminishing after birth. However, recent lineage tracing studies have revealed the presence of tissue-resident macrophages that are produced from early YS precursors independently of HSCs, persist into post-natal life, and are self-maintained without replenishment by BM progenitors (Ginhoux et al., 2010; Gomez Perdiguero et al., 2015; Schulz et al., 2012). These hematopoietic waves are recently recognized as HSC-independent hematopoiesis. Similarly, we and others have reported T and B lymphoid potential in the YS and/or para-aortic splanchnopleura (P-Sp) region prior to HSC emergence by co-culture with stromal cells (Cumano et al., 1996; Godin et al., 1995; Nishikawa et al., 1998; Yoshimoto et al., 2011, 2012). However, it is still controversial whether these T and B cells are produced independently of HSCs because the co-culture system also yields transplantable hematopoietic progenitor/stem cells from as early as E8.0 embryos, which makes the origin of early lymphoid cells unclear, whether it is derived from HSC-independent or -dependent precursors (Cumano et al., 2001; Matsuoka et al., 2001).

This is an open access article under the CC BY-NC-ND license (http://creativecommons.org/licenses/by-nc-nd/4.0/).

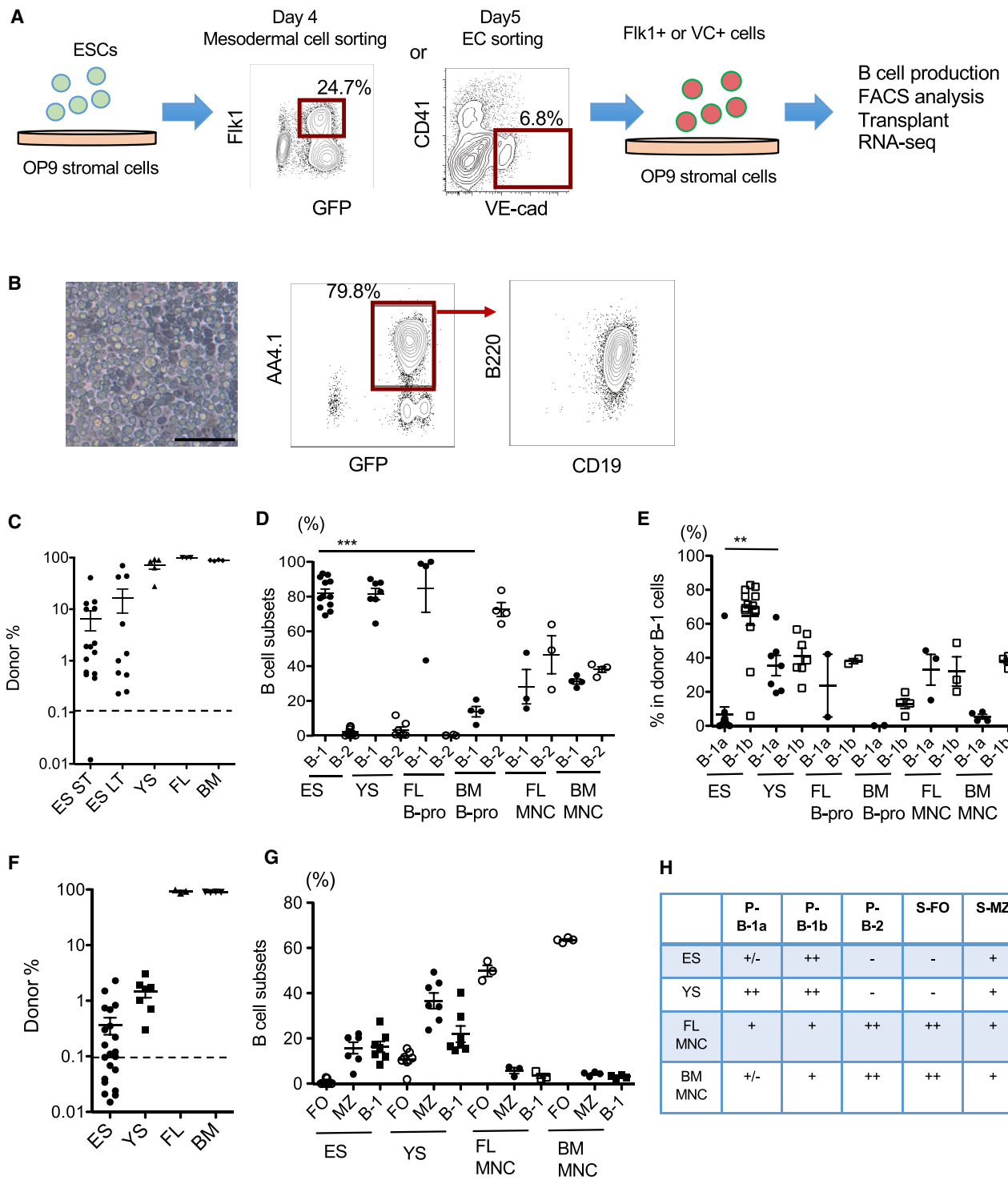

	P-B-1a	P-B-1b	P-B-2	S-FO	S-MZ
ES	+/-	++	-	-	+
YS	++	++	-	-	+
FL MNC	+	+	++	++	+
BM MNC	+/-	+	++	++	+

Figure 1. ESC-Derived B-Progenitors Engraft in the Immunodeficient Mice and Differentiate into B-1 Cells and MZ B Cells, but Not B-2 Cells

(A) A schema for the experimental procedure. Mouse ESCs were differentiated on OP9 into Flk1$^+$ mesodermal cells at day 4 or CD41$^-$VE-cadherin (VC)$^+$ endothelial cells at day 5. The Flk1$^+$ cells or VC$^+$ cells were then re-plated on OP9 with IL-7 and Flt3-ligand for differentiation to B-progenitors. Once AA4.1$^+$CD19$^+$B220$^+$ B-progenitors were obtained at 10–14 days after initiating the co-culture, those B-progenitors were transplanted into sublethally irradiated NSG neonates or a subject of RNA sequencing.

(legend continued on next page)

We previously reported that the earliest B cells produced *in vitro* from YS/P-Sp at pre-HSC stages are B-1 cells (Yoshimoto et al., 2011). B-1 cells are unique innate-like B cells, residing mainly in the pleural and peritoneal cavities, and are segregated from conventional adaptive immune B-2 cells (Baumgarth, 2017). Two subtypes of B-1 cells are categorized; $CD5^+$B-1a cells and $CD5^-$B-1b cells. Among three subsets of B cells (B-1, B-2, and splenic marginal zone [MZ] B cells), B-1 and a part of MZ B cells are considered fetal derived. Especially, $CD5^+$B-1a cells are derived exclusively from progenitors in the fetal liver (FL) and neonatal BM, not from adult HSCs based on the results of transplantation assays (Ghosn et al., 2012; Hardy and Hayakawa, 1991) and a conditional *Rag2* knockout mouse model (Hao and Rajewsky, 2001). Our report demonstrating the presence of B-1-specific progenitors in the FL in HSC-deficient embryos supports the concept of HSC-independent lymphopoiesis (Kobayashi et al., 2014). In addition, the existence of HSC-independent T lymphopoiesis has been recently reported in a zebrafish model (Tian et al., 2017).

Thus, based on our prior results above, we hypothesized that B cells derived from ESCs are also B-1 cells and HSC independent. To test this hypothesis, we induced mouse ESCs on OP9 stromal cells into B-progenitors and transplanted them into sublethally irradiated NOD/SCID/$Il2r\gamma c^{null}$ (NSG) neonates. ESC-derived B cells were detected as peritoneal B-1 cells and splenic MZ B cells in the recipient mice, similar to YS-derived B cells in our previous reports. These B-1 and MZ B cells were maintained in NSG mice for more than 6 months and secreted natural immunoglobulin M (IgM) antibodies *in vivo*. RNA sequencing (RNA-seq) analysis displayed similarity between ESC-derived and YS-derived B-progenitors.

Taken together, our results demonstrate that functional transplantable B-1 cells can be produced in conventional ESC culture and support the existence of HSC-independent B-lymphopoiesis.

RESULTS

Mouse ESC-Derived B-Progenitors Differentiate into Only B-1 and MZ B Cells *In Vivo*

We have previously reported that E9 YS and P-Sp *in vitro* culture produced $AA4.1^+CD19^+B220^+$ B-progenitor cells that differentiate into B-1 cells, but not B-2 cells, *in vivo* after adoptive transfer (Yoshimoto et al., 2011). Based on the fact that ESC differentiation into hematopoietic lineage *in vitro* recapitulates YS hematopoiesis, we hypothesized that B lymphocytes that were produced in the mouse ESC culture were B-1 cells, as was the case for YS-derived B-progenitors. $AA4.1^+CD19^+B220^+$ B-progenitors were differentiated from ESCs via $Flk1^+$ mesoderm or $(VC)^+$ ECs, forming cobblestone areas on OP9 stromal cells as reported previously (Figures 1A and 1B) (Yoshimoto et al., 2009). These $AA4.1^+CD19^+B220^+$ B-progenitors were injected into the peritoneal cavity of sublethally irradiated NSG neonates. Fifty mice were transplanted and 27 mice were analyzed at 5–8 weeks and 23 mice were analyzed at 6 months after transplantation. Fourteen out of 27 mice at 5–8 weeks after transplantation displayed ESC-derived B cells in the peritoneal cavity (Figures 1C and 2A; Table S1). Those B cells were all B-1 cells, not B-2 cells. As expected, ESC-derived B cell subsets were very similar to YS- and FL-derived B cells (Yoshimoto et al., 2011), but not to BM-derived B-progenitors (Figures 1D, 1E, and 1H). Of note, ESC-derived B-progenitors fail to differentiate into B-1a cells (Figures 1E and 2A). ESC-derived MZ B cells and B-1 cells were also detected in the recipient spleen at 5 weeks after transplantation (Figures 1F and 2B; Table S1). ESC-derived B-2 follicular B (FO) cells were not detected, again, similar to the results from YS-derived B cell engraftment (Figures 1G, 1H, and 2B). No thymus was detected in the recipient mice and no myeloid or T cells were detected in the spleen and BM (Figure S1).

(B) Left panel: cobblestone formation of ESC-derived B-progenitors on OP9 culture. Scale bar, 100 μm. Middle and right panels: fluorescence-activated cell sorting (FACS) analysis of the cells forming the cobblestone areas shows $AA4.1^+CD19^+B220^{dim}$ B-1 progenitor phenotype derived from GFP^+ ESCs.

(C) ESC-derived cell ($CD45.2^+$) percentages in the lymphocytes gated population of the recipient peritoneal cells at 5–6 weeks after transplantation (short term [ST], n = 14) and at 6 months after transplantation (long term [LT], n = 10) are depicted.

(D) The percentage of B cell subsets in the donor-derived IgM^+ cells in the peritoneal cavity of recipient mice is shown. ES, ESC-derived B cells; YS, YS-derived B cells; FL-B pro, FL-derived B-progenitors; BM B-pro, adult BM-derived B-progenitors. FL mononuclear cells (MNCs) and BM MNCs were transplanted as a control.

(E) The percentage of B-1a and B-1b cells among the B-1 cells in the recipient peritoneal cavity.

(F) The donor cell (CD45.2+) percentages in the lymphocyte-gated population of the recipient spleen (n = 24 for both ST and LT). The engraftments of YS-derived B-progenitors, FL and BM MNCs are also shown as controls.

(G) The percentages of B cell subsets among donor-derived IgM^+ cells in the recipient spleen are shown. The data were collected from 5 to 6 weeks and 6 months after transplantation. FO, follicular B cells; MZ, marginal zone B cells. Representative FACS plots and surface markers to separate B cell subsets are depicted in Figure 2 and Table S1.

(H) Summary for differentiation capacity of progenitors that are derived from ESC, YS, FL, and BM. P-, peritoneal; S-, spleen.

***$p < 0.0001$, **$p < 0.01$.

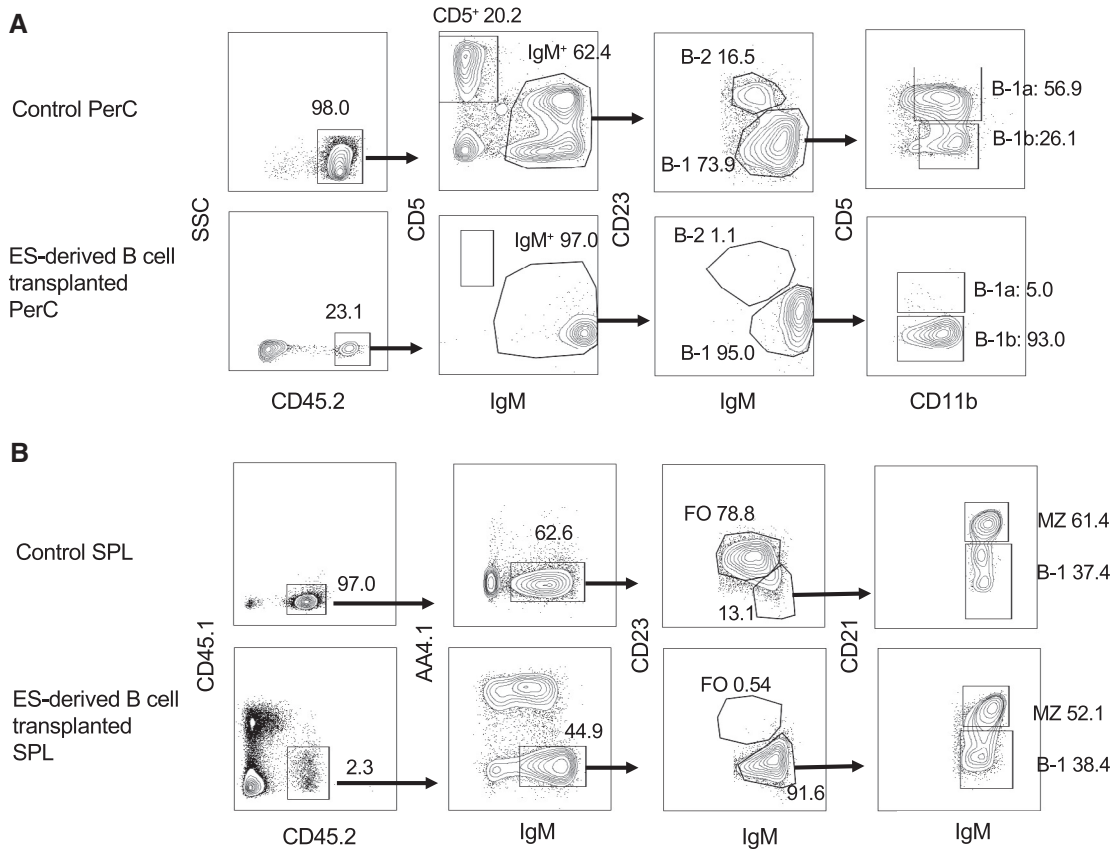

Figure 2. Flow Cytometric Analysis of the Recipient Peritoneal Cells and Spleen

Representative FACS plots for the analysis of peritoneal cells (PerC) (A) and spleen cells (SPL) (B) in the recipient mice transplanted with ESC-derived B-progenitors (AA4.1$^+$CD19$^+$B220$^+$ cells) at 5–6 weeks after transplantation (n = 14) are depicted. Upper panels in (A and B) show FACS plots from non-transplanted C57BL/6 mice. Lower panels in (A and B) show ESC-derived B cell subsets in the PerC (A) and spleen (B) of the transplanted mice, respectively. Surface markers for each B cell subset are listed in Table S1. FO, follicular B cells; MZ, marginal zone B cells.

Thus, only B-1 and MZ B cells were differentiated from ESC-derived B-progenitors in the recipient mice.

ESC-Derived B Cells Display Long-Term Engraftment in the Peritoneal Cavity and Spleen

An important characteristic of B-1 cells is self-replenishing ability. We detected ESC-derived B-1 cell engraftment more than 6 months in 10 out of 23 transplanted mice without engraftment of other lineages (Figures 1C and 3A). ESC-derived B-1 and MZ B cells were also detected in the recipient spleen (Figures 1F, 1G, and 3A). Fat-associated lymphoid clusters (FALCs) have recently been reported as a niche for B-1 cells (Benezech et al., 2015; Moro et al., 2010). Fat tissues were isolated from the recipient peritoneal cavity and stained with anti-IgM antibodies. While non-transplanted NSG mice did not show any IgM$^+$ cells, transplanted NSG mice showed a few, but large, IgM$^+$ clusters in the peritoneal fat tissues (Figure 3B). We also examined ESC-derived IgM$^+$ cells in the recipient spleen. IgM$^+$IgD$^-$ B-1/MZ B cells were confirmed as clusters in the recipient spleen (Figure 3C) although a normal follicular structure was not seen due to lack of T and B-2 cells.

Thus, ESC-derived B-progenitors differentiate into B-1 cells in the peritoneal cavity and MZ B cells in the spleen in the recipient mice and are maintained for more than 6 months.

ESC-Derived B-1 Cells Secrete Natural Antibodies *In Vivo*

To confirm the natural antibody production ability of ESC-derived B-1 cells, we isolated ESC-derived B-1 cells engrafted in the recipient peritoneal cavity and performed ELISpot assays. When the same number of B-1 cells were plated in the plate coated with anti-mouse IgM antibodies, a similar number of spots were observed in ESC-derived B-1 cells and control C57 BL/6 B-1 cells, but not in B-2 cells

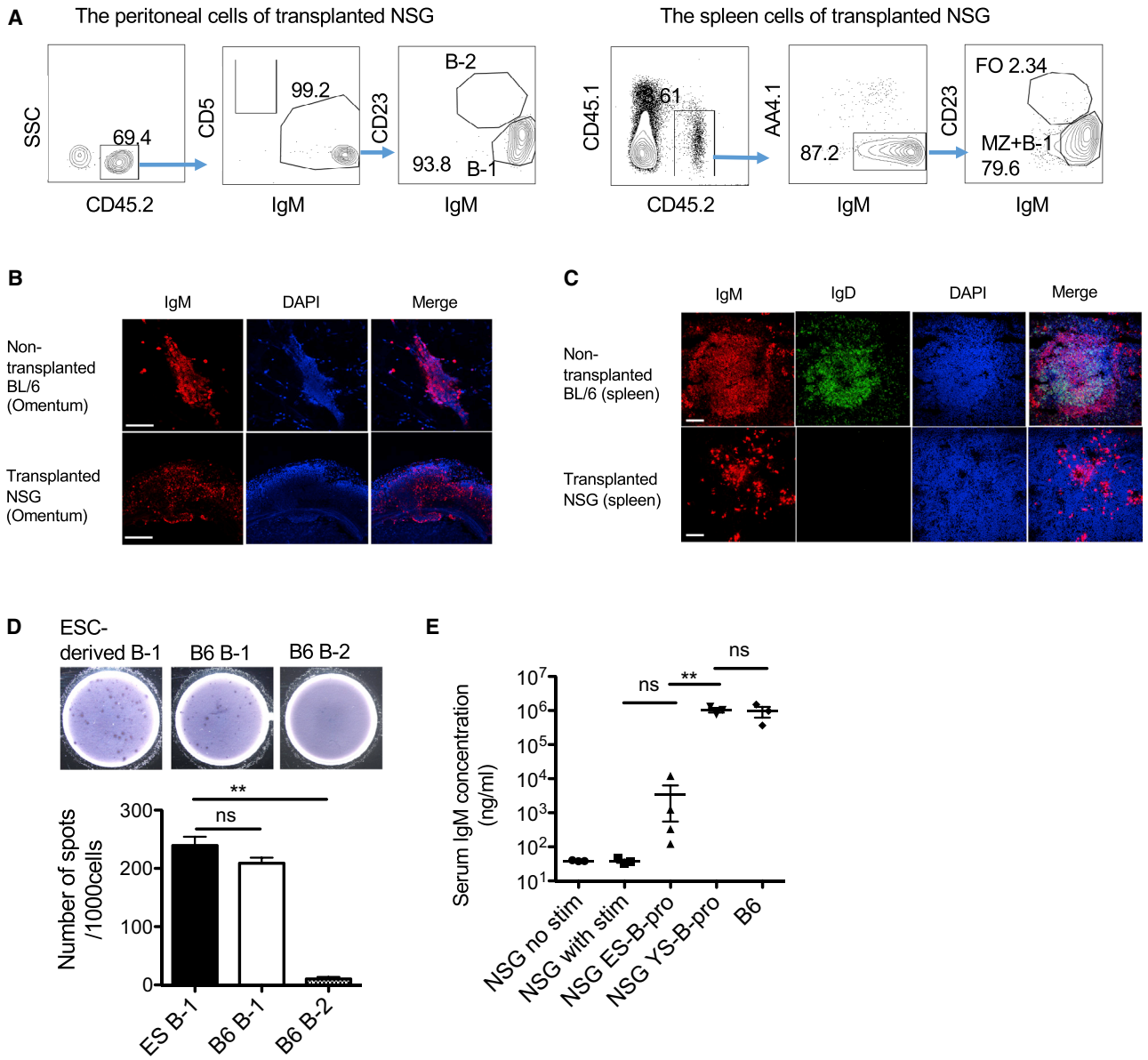

Figure 3. ESC-Derived B-1 Cells Are Functional to Secrete Natural Antibodies and Maintained in the Recipient Mice

(A) ESC-derived B cell subsets in the peritoneal cavity and spleen from the recipient NSG mice at 6 months after transplantation with AA4.1$^+$CD19$^+$B220$^+$ B-progenitors. Representative FACS plots are depicted among ten transplanted mice. FO, follicular B cells; MZ, marginal zone B cells.

(B) Immunostaining of FALCs in non-transplanted C57BL/6 (B6) mice (control) and the recipient mice after phosphorylcholine (PC) stimulation (n = 3). Red, anti-IgM antibody; blue, DAPI. Scale bars, 100 μm (upper panel) and 200 μm (lower panel).

(C) Immunostaining of spleen in non-transplanted B6 mice (control) and the recipient mice after PC stimulation (n = 3). Green, anti-IgD antibody; red, anti-IgM antibody; blue, DAPI. Scale bar, 100 μm.

(D) ELISpot assays against anti-PC IgM using 1,000 ESC-derived B-1 cells harvested from the peritoneal cavity of transplanted mice, and 1,000 B-1 and B-2 cells harvested from the B6 peritoneal cavity (n = 3 for each group).

(E) Concentrations of serum IgM from non-transplanted NSG with or without PC stimulation, NSG mice transplanted with ESC- or YS-derived B-progenitors, and non-treated B6 mice are depicted. All transplanted mice were stimulated with PC before collecting the serum (n = 3 for each group).

**p < 0.01.

(Figure 3D). Phosphorylcholine was injected into the mice transplanted with ESC-derived B cells and the serum IgM was measured by enzyme-linked immunosorbent assay (ELISA) assays (Figure 3E). The control mice transplanted with YS-derived B cells displayed similar levels of serum IgM to non-transplanted C57BL/6 mice. The recipient NSG mice transplanted with ESC-derived B cells showed elevated IgM levels compared with non-transplanted NSG mice, although less than non-transplanted C57BL/6 serum IgM or YS-derived serum IgM. The difference in IgM level between mice transplanted with ESC- and YS-derived B cells might depend on the cell numbers engrafted in the host mice. Thus, ESC-derived B-1 cells are functional IgM-secreting cells *in vivo*.

Gene Expression Profile of ESC-Derived B-Progenitors Is Similar to that of YS- and FL-Derived B-1 Progenitors

We compared gene expression profiles among ESC-, YS-, and FL-derived B-1 progenitors and BM-derived B-2 progenitors to evaluate molecular similarities (Figure 4A). Principal-component analysis showed that ESC-derived B-progenitors are molecularly closer to YS- and FL-derived B-1 progenitors rather than BM-derived B-2 progenitors, as expected (Figure 4B). However, there were 1,759 genes differentially expressed between ESC-derived and YS-derived B-1 progenitors ($p < 0.05$, false discovery rate [FDR] < 0.05, >2-fold). Among them, 715 genes were upregulated and 1,044 genes were downregulated in ESC-derived B-progenitors compared with YS-derived B-progenitors. On the other hand, 4,805 genes were differentially expressed between ESC- and BM-derived B-progenitors (2,479 genes were upregulated, and 2,326 genes were downregulated in ESC-derived B-progenitors, $p < 0.05$, FDR < 0.05, >2-fold).

Careful evaluation of the transcription factors important for B cell development revealed that ESC-derived B-progenitors were similar to those of YS- or FL-derived B-progenitors (Figure 4C). Since FL-derived B-progenitors include some cells with B-2 potential, expression was at times similar to BM-derived B cells, depending on the genes. *Lmo2*, *Spi1 (PU.1)*, *Pax5*, *Ebf1*, and *Ikzf1* were expressed higher in BM-derived B-progenitors than ESC-, YS-, and FL-derived B-1 progenitors, while *Rag2* and *Bcl11a* were expressed higher in the ESC-, YS-, and FL-derived B-progenitors (Figure 4C). Expression patterns of chemokine receptors showed a distinct difference between YS/FL-derived B-1 progenitors and BM-derived B-2 progenitors, and those chemokine receptors appeared to be silent in ESC-derived B-progenitors (Figure 4D). Among them, *Ccr7* and *Cxcr5* were expressed differently between ESC-derived and YS/FL-derived B-progenitors. CXCR5 is an important homing receptor for B-1 cells that promotes retention in the peritoneal cavity (Hopken et al., 2004), thus this difference could account for the lower efficiency of ESC-derived B cell engraftment in the recipient mice. Expression of some cytokine receptors was also reduced in the ESC-derived B-progenitors (Figure 4E). We also looked into genes involved in epigenetic modification (Figure 4F). We confirmed that ESC-derived B-progenitors showed lower expression of *Bmi1* and *Rnf2 (Ring1B)*, an important component of polycomb repressive complex 1. We performed gene ontogeny (GO) enrichment analysis between ESC- and YS-derived B-progenitors and identified the top 10 categories of upregulated genes in YS-derived B-progenitors (Figure 4G) and in ESC-progenitors (Figure 4H). While MHC protein complex and interferon-γ signaling pathways were upregulated in the YS-derived B-1 progenitors, some mesodermal developmental signatures were still upregulated in the ESC-derived B-1 progenitors. Taken together, ESC-derived B-1 progenitors may not be fully developed, although B cell transcription factors are similar between YS- and ESC-derived B-1 progenitors. Nonetheless, engrafted ESC-derived B-1 cells were immunologically functional; thus, some ESC-derived B-progenitors might be selected *in vivo* or these differences may reflect the lack of B-1a cells from ESC-derived B-1 progenitors.

Bmi1 Overexpression Improved ESC-Derived B-1 Cell Engraftment

Since *Bmi1* expression was reduced in ESC-derived B-progenitors (Figure 4F) and *Bmi1* overexpression is reported to increase the self-renewal capacity of HSCs and self-renewing YS-derived erythroid progenitor cells (Iwama et al., 2004; Kim et al., 2015), we hypothesized that overexpression of *Bmi1* might improve ESC-derived B cell engraftment. qPCR showed less *Bmi1* expression in ESC-derived B-progenitors compared with YS-derived B-progenitors (Figure 5A). Therefore, we overexpressed *Bmi1* in ESCs by retrovirus, differentiated them into B-progenitors on OP9, and transplanted $AA4.1^+CD19^+B220^+$ B-progenitors into sublethally irradiated NSG neonates as described above. Elevated *Bmi1* expression was confirmed by qPCR (Figure 5A). In the recipient peritoneal cavity, *Bmi1*-overexpressing B cells demonstrated significantly better engraftment at 4–5 weeks (Figure 5B, $n = 8$, average donor $26.6\% \pm 21.3\%$, $p = 0.01$), and at 4 months after transplantation (Figure 5C, $n = 7$, average donor $21.4\% \pm 16\%$, $p < 0.05$) compared to parent ESC-derived B cells ($n = 5$, $0.73\% \pm 0.58\%$ at 5 weeks, $n = 3$, $4.3\% \pm 2.1\%$ at 4 months). Of note, despite improved engraftment, ESC-derived B-1a cells were not detected (Figure 5D).

We also examined CXCR5 expression in differentiated ESC-derived IgM^+ cells on OP9 culture because CXCR5 is an essential chemokine receptor expressed in the peritoneal B-1 cells and *Cxcr5* deletion induced B-1 cell loss in the peritoneal cavity (Hopken et al., 2004). We confirmed CXCR5 expression in B-1 cells of non-transplanted

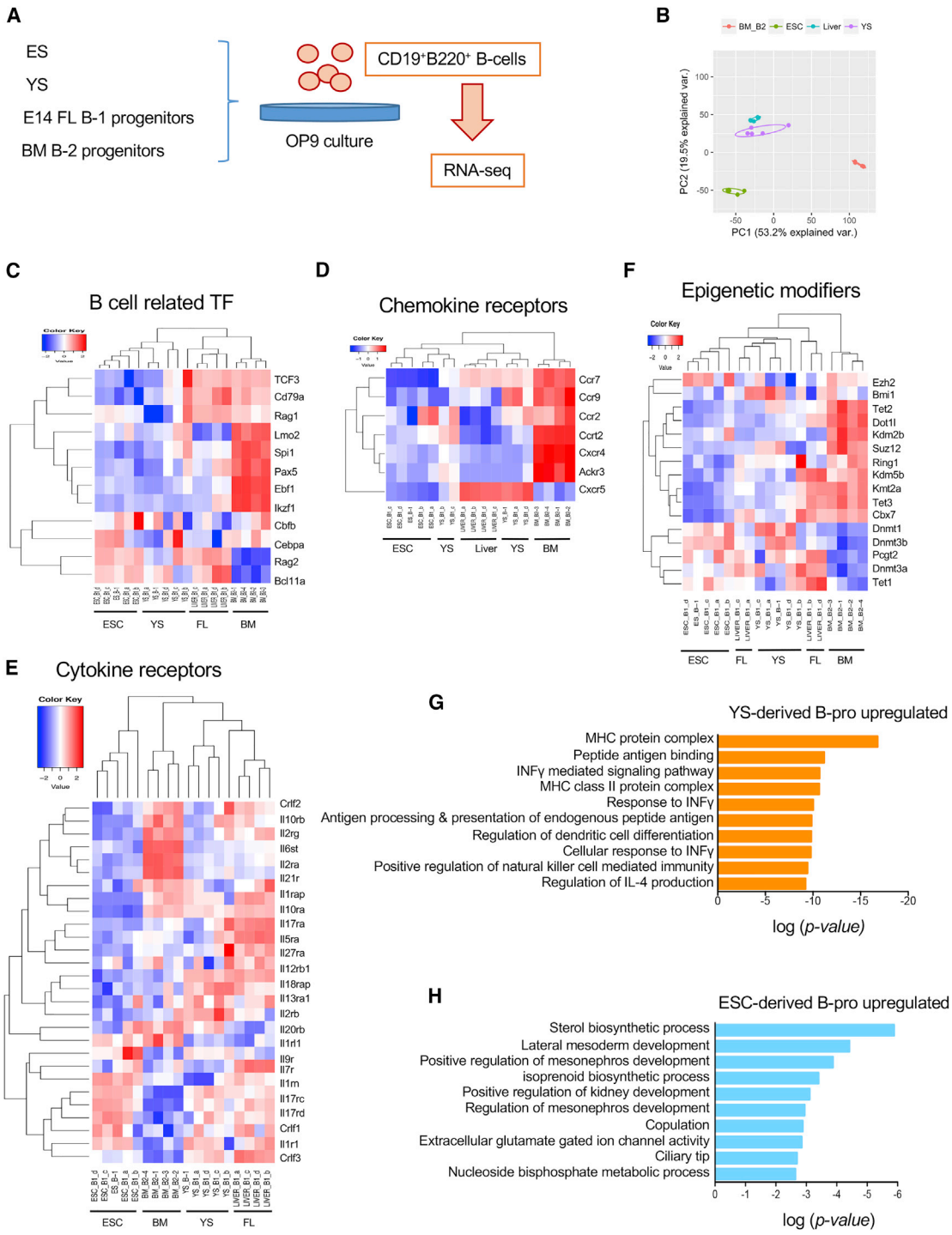

Figure 4. The Gene Expression Profile of ESC-Derived B-1 Cells Is Similar to that of YS- and FL-Derived B-1 Cells

(A) An experimental procedure.

(B) Principal-component analysis of RNA sequencing profiles among ESC-, YS-, FL-, and BM-derived B-progenitors.

(C–F) Heatmap analysis among ESC-, YS-, FL-, and BM-derived B-progenitors for B cell-related transcription factors (C), chemokine receptors (D), cytokine receptors (E), and epigenetic regulatory genes (F).

(G and H) The top 10 categories of upregulated genes in YS-derived B-progenitors (G) and ESC-progenitors (H) between these two populations by gene ontology enrichment analysis are listed. B-pro, B-progenitors

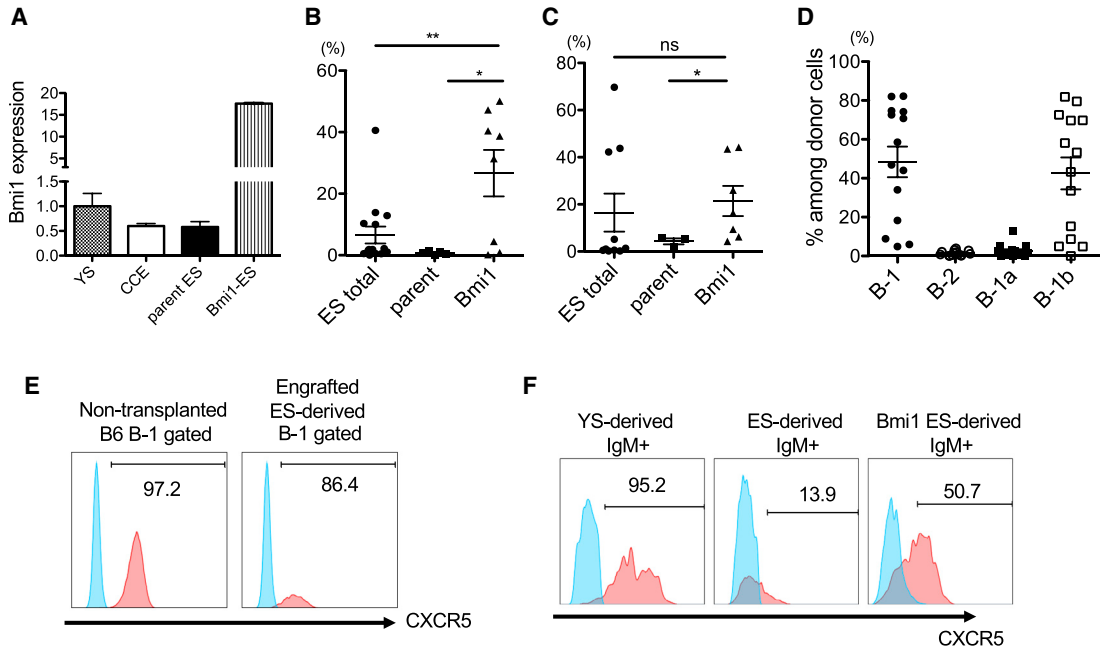

Figure 5. Overexpressing *Bmi1* Improved ESC-Derived B-1 Cell Engraftment

(A–C) *Bmi1* expression in B cells produced *in vitro* from YS, CCE (ES), parent ES, and Bmi1-expressing ESCs (A). The percentages of donor-derived B cells in the peritoneal cavity (lymphocyte-gated) of the recipient mice at 5 weeks (B) and 4 months (C) after transplantation with AA4.1$^+$CD19$^+$B220$^+$ B-progenitors derived from regular ESCs (ES total, left), parent ESCs (middle), and *Bmi1*-expressing-ESCs (right) are shown.

(D) B cell subsets derived from *Bmi1*-expressing ESCs engrafted in the recipient peritoneal cavity.

(E) CXCR5 expression (pink) in non-transplanted B6 B-1 cells and engrafted ES-derived B-1 cells. Blue population is fluorescent-minus-one for CXCR5 as a negative control.

(F) CXCR5 expression (pink) in IgM$^+$ B cells differentiated from YS, parent ESCs, and *Bmi1*-ESCs on OP9 culture. Blue is CXCR5-negative population. Representative histograms are depicted (n = 3 for each group).

**$p < 0.01$, *$p < 0.05$.

C57BL/6 mice and ESC-derived B-1 cells engrafted in NSG mice (Figure 5E). However, in *in vitro* differentiation on OP9, IgM$^+$ cells from parent ESCs was not efficiently produced and showed less CXCR5 expression, while YS and *Bmi1*-ESCs differentiated into CXCR5-expressing IgM$^+$ cells at 3 weeks after differentiation (Figure 5F). These results suggested that the differentiation efficiency into CXCR5$^+$IgM$^+$ cells may be a key for ESC-derived B-progenitors to engraft in the recipient peritoneal cavity. Further studies have to be done to enhance the engraftment of ESC-derived B-progenitors.

DISCUSSION

We demonstrated that all B-progenitors produced from mouse ESCs differentiate into only B-1 and MZ B cells in recipient mice, similar to YS-derived B-progenitors (Figure 1H). Although ESC-derived B-1 cells are functional in natural antibody secretion and self-replenishing ability, they differentiate to mostly B-1b cells, not to B-1a cells, while almost half of YS-derived B-progenitors differentiate into B-1a cells *in vivo* (Figure 1E) (Yoshimoto et al., 2011). This may reflect the difference of gene expression between ESC- and YS-derived B-progenitors. Although ESC-derived B-progenitors are molecularly more similar to YS-derived B-progenitors than BM B-2 progenitors, there were still 1,759 genes differentially expressed between them. Potocnik et al. (1997) have reported B cell reconstitution by *in vitro* differentiated mouse ESCs, including both B-1 and transient B-2 cells. While B-1a cells were dominantly repopulated in their report, our ESC-derived cells repopulated only B-1b cells and not B-2 cells. This difference may be due to dissimilarity in culture conditions such as 3D embryoid body formation versus 2D OP9 co-culture. In both cases, however, HSCs that could sustain B-2 cell production were not detected.

We have previously shown that mouse testis-derived PSCs differentiate into erythromyeloid progenitors, and B and T cells *in vitro* culture, but found very limited

PSC-derived HPC engraftment in the recipient BM and spleen, detectable by PCR (Yoshimoto et al., 2009). Pearson et al. (2015) have reported better engraftment of ESC-derived hematopoietic cells after serum-free differentiation culture. However, despite T cell differentiation potential *in vitro*, T cell engraftment was not shown and B cell engraftment was limited to the spleen. They indicated that the engrafted B cells in the recipient spleen were not B-1 cells because they lacked expression of CD5 and CD11b. However, CD11b is only expressed in peritoneal B-1 cells, not in splenic B-1 cells. Furthermore, CD5 expression is limited to B-1a cells. Since they did not show any B cell engraftment in the peripheral blood (which is considered to represent the B-2 cell population), it is very likely that the ESC-derived B cells engrafted in the recipient spleen were MZ or B-1 cells, consistent with our results.

Lu et al. (2016) have reported repopulation of functional adaptive immune T and B cells by engineered mouse ESCs, which was produced by inducing Notch signaling and *Hoxb4* overexpression. In their control, conventional ESC differentiation on OP9 (without Notch signaling) produced only B-1b cells, not B-2 cells, supporting our results. Notch signaling seems to have induced functional adaptive B-2 cells via HSCs in their system, although their secondary transplantation of engineered HSCs displayed T cell dominant engraftment. This result suggests that sustained B-2 potential always accompanies HSC potential, different from B-1 cells that can be produced by early HSC-independent progenitors. Although lymphoid potential has been used as an indicator of "definitive hematopoiesis" in the early mouse embryo or ESC differentiation system (Cumano et al., 1996; Kennedy et al., 2012), it is important to reconsider the definition of definitive hematopoiesis, because some T and B-1 lymphoid progenitors can be produced in the absence of HSCs (Chen et al., 2011; Kobayashi et al., 2014; Tian et al., 2017). In this sense, sustained B-2 cell production may be a more accurate indicator of HSC activity. Therefore, understanding how B-2 potential is obtained in ESC-derived HPCs would represent an important area of future investigation.

RNA-seq results also support the similarity between ESC- and YS-derived B-1 progenitors. *Bmi1* expression, known as an important gene for self-renewal ability in stem cells, was reduced in ESC-derived B cells compared with YS-derived B cells, and *Bmi1* overexpression improved the engraftment of ESC-derived B cells in the recipient mice. Our result is similar to the report that inducing *Bmi1* into adult BM erythroblasts enhanced self-renewal ability extensively (Kim et al., 2015). Thus, *Bmi1* may also play a role in the self-renewal ability of B-1 cells.

Of note, there was a variation of engraftment efficiency among B cells derived from regular ESCs (Figures 1C, 5B, and 5C ES total). Since B-progenitors differentiate into mature IgM$^+$ cells by interacting stromal cells and cytokines in the BM and spleen, the differentiation capacity and characteristics of each ESC line could be important factors for the engraftment, and *Bmi1*-overexpression may have helped this differentiation process as was seen *in vitro* experiments (Figure 5F).

The clinical importance of human B-1 cells has attracted attention based on the methods to isolate the human counterpart of mouse B-1 cells (Griffin et al., 2011; Griffin and Rothstein, 2011). Since BM HSCs do not reconstitute B-1a cells, patients after BM transplantation may lack B-1 cells if human B-1 cells have similar characteristics with mouse B-1 cells. Indeed, it has been reported that patients who develop graft versus host disease following stem cell transplantation are at high risk for developing sepsis from encapsulated bacteria, associated with deficiency of human B-1-like cells that normally produce natural antibodies to these bacteria (Moins-Teisserenc et al., 2013). Therefore, PSC-derived B-1 cells could theoretically be an important source of cell therapy for these patients in the future.

In summary, our data indicate the successful engraftment of ESC-derived functional B-1 cells without gene modifications, supporting the presence of HSC-independent lymphopoiesis and suggesting possible unique applications for cell therapy in the future.

EXPERIMENTAL PROCEDURES

Mice

NSG mice (CD45.1) and C57BL/6 mice (CD45.2) were maintained at the Indiana University Laboratory Animal Resource Center and the Center for Laboratory Animal Medicine and Care at Institute of Molecular Medicine, University of Texas Health Science Center at Houston (UTHealth). All animal experiments were conducted according to the Guidelines for the Care and Use of Laboratory Animals under the guidance of Institutional Animal Care and Use Committees at Indiana University School of Medicine and for the Animal Welfare Committee at UTHealth at Houston.

Flow Cytometry and Magnetic-Activated Cell Sorting

Different fluorochrome-conjugated following antibodies (all purchased from eBioscience) were used for the flow cytometry analysis and sorting: anti-mouse Flk1 (clone Avas12a1), CD144 (11D4.1), CD19 (eBio1D3), B220 (RA3-6B2), AA4.1 (AA4.1), IgM (11/41), CD23 (B3B4), CD11b (M1/70), CD5 (53-7.3), CD45.1 (A20), CD45.2 (104), CD44 (1M7), CD41 (eBioMWReg30), CD25 (PC61), Thy1.2 (53-2.1), CD3 (145-2C11). Propidium iodide (PI) (Sigma-Aldrich) was used for live cell gating. Stained cells were analyzed or sorted on LSRII, FACSCantoII, or FACSAria instrument (BD). Flow cytometry data were analyzed in FlowJo software.

For magnetic-activated cell sorting, CD19$^+$ cells were separated following the manufacturer's instructions using anti-mouse CD19 antibody and anti-Rat IgG MicroBeads (Miltenyi Biotech). The purity of sorted CD19$^+$ cells was >95%, confirmed by flow cytometry.

For BM B-progenitor isolation, $IgM^{-}AA4.1^{+}CD19^{+}B220^{+}$ B-2 progenitors were sorted on FACSAria.

OP9 Cells and ESCs

OP9 stromal cells were provided by Dr. Toru Nakano at Osaka University. ESC lines such as D3, D4, and E14 were kindly provided by Dr. Toshio Heike (retired from Kyoto University). OP9 and ESCs were maintained as described previously (Yoshimoto et al., 2009).

B Cell Differentiation and Transplantation

B cells were differentiated from ESCs as described previously (Yoshimoto et al., 2009). In brief, day 4 $Flk1^{+}$ or day 5 VC^{+} cells of ESC differentiation culture were sorted and re-plated on fresh OP9 monolayers in 6-well culture plates at a density of 3,000–5,000 cells/well and were cultured for an additional 10–14 days in induction medium with 10 ng/mL interleukin-7 (IL-7) and Flt3-ligand (PeproTech).

B cells were differentiated from E9.5 YS as described previously (Yoshimoto et al., 2011).

To obtain FL- and BM-derived B cells, $CD19^{+}$ B-progenitors from E14.5 FL or $CD19^{+}B220^{+}$ B-progenitors from adult BM were sorted and cultured on OP9 for 6 days with 10 ng/mL IL-7 and Flt3-ligand. After cobblestone-like B cell colonies were formed in the culture, the cells were collected. $AA4.1^{+}CD19^{+}B220^{+}$ cells were then sorted by FACSAria (Becton Dickinson) and were used for downstream experiments or kept in liquid nitrogen as cell pellets for RNA-seq.

For cell transplantation, donor cells were re-suspended in 25 μL PBS and were injected into the peritoneal cavity of sublethally (150 rad) irradiated NSG neonates (1–3 days old). At different time points after transplantation, the peritoneal, spleen or BM cells were collected and donor cell types were examined by flow cytometry.

Images and Confocal Microscopy

Pictures of cell culture were taken on a Leica DM IL microscope with a SPOT RT3 camera (Spot Imaging). For confocal microscopy images of FALCs, recipient NSG were euthanized, and omentum and mesenteric fat tissues were dissected. The samples were prepared as described previously (Benezech et al., 2015) and stained with 1:200 Alexa Fluor 555-conjugated anti-mouse IgM antibody (SouthernBiotech). Confocal images were taken using an Olympus II microscope with UApoN340 20×/0.7W objectives (Olympus). ImageJ software was used to adjust and output the images.

Natural Antigen Immunization and ELISA

To measure the serum IgM concentration after natural antigen challenge, mice were immunized by intraperitoneal injection of 200 μL 0.25 mg/mL phosphorylcholine conjugated to keyhole limpet hemocyanin (PC-KLH). After 10 days, the mice were euthanized and blood serum was used for IgM ELISA assay using eBioscience Mouse IgM ELISA Ready-SET-Go! Kit according to the manufacturer's instructions.

ELISpot

ELISpot assays were performed as described previously (Kobayashi et al., 2014). In brief, B cells were sorted from the peritoneal cavity or spleen of recipient or control animals by FACSAria (BD Bioscience). The cells were re-suspended in RPMI 1640 medium with 10% fetal bovine serum, 5×10^{-5} M β-mercaptoethanol, and 10 ng/mL IL-5 (PeproTech) and plated on 96-well plates that were pre-coated with 10 μg/mL PC-KLH. After 24 h incubation, the cells were collected and re-plated into each well of ELISpot $Multiscreen_{HTS}$ Filter Plates (Millipore) pre-coated with 10 μg/mL anti-mouse IgM antibody (eBioscience). After 24 h, the wells were incubated with 1:2,000 alkaline phosphate-conjugated goat anti-IgM detection antibody (SouthernBiotech) and the spots were visualized by BCIP/NBT-plus substrate (Mabtech). Photos of spots were taken using a Zeiss Stemi SV 11 microscope with Zeiss Axiocam Mrc5 camera.

RNA-Seq

Cell pellets of sorted B-progenitors derived from ESCs, E9.5 YS, E14.5 FL, and adult BM were snap-frozen in liquid nitrogen and stored at −80°C before RNA isolation. RNA was isolated using RNeasy MicroMini Kit (QIAGEN) and submitted to the Center for Medical Genomics at IUSM for the RNA-seq. Total RNA was first evaluated for its quantity and quality, using an Agilent Bioanalyzer. Starting amount of total RNA ranged from 200 to 1,000 ng for library preparation. Ribosomal RNA was first removed from total RNA using a standard protocol for the Ribo-Zero Magnetic Gold Kit (Epicentre, cat. no. MRZG12324/RZG1224). After the depletion of rRNA, cDNA library preparation included enzymatic fragmentation, hybridization, and ligation of adaptors, reverse transcription, size selection, and amplification with barcode primers, following the Ion Total RNA-Seq Kit v.2 User Guide, Pub. no. 4476286 Rev. E (Life Technologies). Each resulting barcoded library was quantified and its quality assessed by Agilent Bioanalyzer and multiple libraries pooled in equal molarity. Eight microliters of 100 pM pooled libraries were then applied to Ion Sphere Particles (ISP) template preparation and amplification using Ion OneTouch 2 (Life Technologies), followed by ISP loading onto a PI chip and sequencing on Ion Proton semiconductor (Life Technologies). Each PI chip allowed loading of about 140 million ISP templates, generating approximately 80–100 million usable reads, up to 10–15 Gb.

Bioinformatic Analysis

RNA-seq was carried out using a standard RNA-seq protocol by Ion Proton technology in the Center for Medical Genomics, Indiana University. The sequencing data were mapped to the *Mus musculus* mm10 reference genome using RNA-seq aligner STAR (v.2.4.2) (Dobin et al., 2013). The gene-based expression levels were quantified with featureCounts (subread v.1.5.0) (Liao et al., 2014) applying parameters "-s 1 –Q 10." Read counts were normalized to the total number of sequencing reads falling into annotated gene regions in each sample, and further scaled based on a trimmed mean of log transformed counts per million (CPM) value to correct for the variability of RNA composition in each sample. The genes with greater than one read per million mappable reads (CPM > 1) in at least four samples were kept for gene differential expression analysis with the R/Bioconductor package edgeR (Robinson et al., 2010). Benjamini and Hochberg's algorithm was used to control the FDR. Gene set enrichment analysis was performed on the C2 curated gene sets and the C5 GO gene sets of the Molecular Signature Database using the function CAMERA in edgeR (Robinson et al., 2010).

Overexpressing *Bmi1* in ESCs

Mouse *Bmi1* cDNA was cloned into pMIPTcG (pMIEG3-IRES-puroR/T2A/GFP) and the sequence was confirmed. Subsequently, virus was produced with Phoenix-Eco producer line by a standard method (Kobayashi et al., 2017). ESCs were infected with pMIPTcG-Mock or -*Bmi1* virus, followed by selection with puromycin.

Statistics

The unpaired, two-tailed Student's t test was used for statistical analysis in this study.

RNA-Seq Accession Number

RNA-seq data are available in the GEO under accession number, GSE123809.

SUPPLEMENTAL INFORMATION

Supplemental Information includes one figure and two tables and can be found with this article online at https://doi.org/10.1016/j.stemcr.2019.01.006.

AUTHOR CONTRIBUTIONS

M.Y. conceived and performed the experiments, analyzed the data, and wrote the manuscript. M.C.Y. conceived the project, analyzed the data, and edited the manuscript. Y. Lin and M.K. performed the experiments, analyzed the data, and edited the manuscript. N.A.P and A.M. performed the experiments. G.H. and Y. Liu performed bioinformatics analysis. B.D. and P.W. discussed the data analysis and edited the manuscript.

ACKNOWLEDGMENTS

We thank the Center for Medical Genomics at IUSM for the RNA sequencing. This work is supported by NIH grant R56AI110831 and R01AI121197 (to M.Y.) and R01DK111599 (to P.W).

Received: May 13, 2018
Revised: January 9, 2019
Accepted: January 10, 2019
Published: February 7, 2019

REFERENCES

Amabile, G., Welner, R.S., Nombela-Arrieta, C., D'Alise, A.M., Di Ruscio, A., Ebralidze, A.K., Kraytsberg, Y., Ye, M., Kocher, O., Neuberg, D.S., et al. (2013). In vivo generation of transplantable human hematopoietic cells from induced pluripotent stem cells. Blood *121*, 1255–1264.

Baumgarth, N. (2017). A hard(y) look at B-1 cell development and function. J. Immunol. *199*, 3387–3394.

Benezech, C., Luu, N.T., Walker, J.A., Kruglov, A.A., Loo, Y., Nakamura, K., Zhang, Y., Nayar, S., Jones, L.H., Flores-Langarica, A., et al. (2015). Inflammation-induced formation of fat-associated lymphoid clusters. Nat. Immunol. *16*, 819–828.

Chen, M.J., Li, Y., De Obaldia, M.E., Yang, Q., Yzaguirre, A.D., Yamada-Inagawa, T., Vink, C.S., Bhandoola, A., Dzierzak, E., and Speck, N.A. (2011). Erythroid/myeloid progenitors and hematopoietic stem cells originate from distinct populations of endothelial cells. Cell Stem Cell *9*, 541–552.

Cumano, A., Dieterlen-Lievre, F., and Godin, I. (1996). Lymphoid potential, probed before circulation in mouse, is restricted to caudal intraembryonic splanchnopleura. Cell *86*, 907–916.

Cumano, A., Ferraz, J.C., Klaine, M., Di Santo, J.P., and Godin, I. (2001). Intraembryonic, but not yolk sac hematopoietic precursors, isolated before circulation, provide long-term multilineage reconstitution. Immunity *15*, 477–485.

Dobin, A., Davis, C.A., Schlesinger, F., Drenkow, J., Zaleski, C., Jha, S., Batut, P., Chaisson, M., and Gingeras, T.R. (2013). STAR: ultrafast universal RNA-seq aligner. Bioinformatics *29*, 15–21.

Ghosn, E.E., Yamamoto, R., Hamanaka, S., Yang, Y., Herzenberg, L.A., Nakauchi, H., and Herzenberg, L.A. (2012). Distinct B-cell lineage commitment distinguishes adult bone marrow hematopoietic stem cells. Proc. Natl. Acad. Sci. U S A *109*, 5394–5398.

Ginhoux, F., Greter, M., Leboeuf, M., Nandi, S., See, P., Gokhan, S., Mehler, M.F., Conway, S.J., Ng, L.G., Stanley, E.R., et al. (2010). Fate mapping analysis reveals that adult microglia derive from primitive macrophages. Science *330*, 841–845.

Godin, I., Dieterlen-Lievre, F., and Cumano, A. (1995). Emergence of multipotent hemopoietic cells in the yolk sac and paraaortic splanchnopleura in mouse embryos, beginning at 8.5 days postcoitus. Proc. Natl. Acad. Sci. U S A *92*, 773–777.

Gomez Perdiguero, E., Klapproth, K., Schulz, C., Busch, K., Azzoni, E., Crozet, L., Garner, H., Trouillet, C., de Bruijn, M.F., Geissmann, F., et al. (2015). Tissue-resident macrophages originate from yolk-sac-derived erythro-myeloid progenitors. Nature *518*, 547–551.

Griffin, D.O., Holodick, N.E., and Rothstein, T.L. (2011). Human B1 cells in umbilical cord and adult peripheral blood express the novel phenotype CD20+ CD27+ CD43+ CD70. J. Exp. Med. *208*, 67–80.

Griffin, D.O., and Rothstein, T.L. (2011). A small CD11b(+) human B1 cell subpopulation stimulates T cells and is expanded in lupus. J. Exp. Med. *208*, 2591–2598.

Hadland, B., and Yoshimoto, M. (2017). Many layers of embryonic hematopoiesis: new insights into B cell ontogeny and the origin of hematopoietic stem cells. Exp. Hematol. *60*, 1–9.

Hao, Z., and Rajewsky, K. (2001). Homeostasis of peripheral B cells in the absence of B cell influx from the bone marrow. J. Exp. Med. *194*, 1151–1164.

Hardy, R.R., and Hayakawa, K. (1991). A developmental switch in B lymphopoiesis. Proc. Natl. Acad. Sci. U S A *88*, 11550–11554.

Hopken, U.E., Achtman, A.H., Kruger, K., and Lipp, M. (2004). Distinct and overlapping roles of CXCR5 and CCR7 in B-1 cell homing and early immunity against bacterial pathogens. J. Leukoc. Biol. *76*, 709–718.

Irion, S., Clarke, R.L., Luche, H., Kim, I., Morrison, S.J., Fehling, H.J., and Keller, G.M. (2010). Temporal specification of blood progenitors from mouse embryonic stem cells and induced pluripotent stem cells. Development *137*, 2829–2839.

Iwama, A., Oguro, H., Negishi, M., Kato, Y., Morita, Y., Tsukui, H., Ema, H., Kamijo, T., Katoh-Fukui, Y., Koseki, H., et al. (2004). Enhanced self-renewal of hematopoietic stem cells mediated by the polycomb gene product Bmi-1. Immunity *21*, 843–851.

Kennedy, M., Awong, G., Sturgeon, C.M., Ditadi, A., LaMotte-Mohs, R., Zuniga-Pflucker, J.C., and Keller, G. (2012). T lymphocyte potential marks the emergence of definitive hematopoietic progenitors in human pluripotent stem cell differentiation cultures. Cell Rep. *2*, 1722–1735.

Kim, A.R., Olsen, J.L., England, S.J., Huang, Y.S., Fegan, K.H., Delgadillo, L.F., McGrath, K.E., Kingsley, P.D., Waugh, R.E., and Palis, J. (2015). Bmi-1 regulates extensive erythroid self-renewal. Stem Cell Reports *4*, 995–1003.

Kobayashi, M., Nabinger, S.C., Bai, Y., Yoshimoto, M., Gao, R., Chen, S., Yao, C., Dong, Y., Zhang, L., Rodriguez, S., et al. (2017). Protein tyrosine phosphatase PRL2 mediates notch and kit signals in early T cell progenitors. Stem Cells *35*, 1053–1064.

Kobayashi, M., Shelley, W.C., Seo, W., Vemula, S., Lin, Y., Liu, Y., Kapur, R., Taniuchi, I., and Yoshimoto, M. (2014). Functional B-1 progenitor cells are present in the hematopoietic stem cell-deficient embryo and depend on Cbfbeta for their development. Proc. Natl. Acad. Sci. U S A *111*, 12151–12156.

Kyba, M., Perlingeiro, R.C., and Daley, G.Q. (2002). HoxB4 confers definitive lymphoid-myeloid engraftment potential on embryonic stem cell and yolk sac hematopoietic progenitors. Cell *109*, 29–37.

Liao, Y., Smyth, G.K., and Shi, W. (2014). featureCounts: an efficient general purpose program for assigning sequence reads to genomic features. Bioinformatics *30*, 923–930.

Lin, Y., Yoder, M.C., and Yoshimoto, M. (2014). Lymphoid progenitor emergence in the murine embryo and yolk sac precedes stem cell detection. Stem Cells Dev. *23*, 1168–1177.

Lu, Y.F., Cahan, P., Ross, S., Sahalie, J., Sousa, P.M., Hadland, B.K., Cai, W., Serrao, E., Engelman, A.N., Bernstein, I.D., et al. (2016). Engineered murine HSCs reconstitute multi-lineage hematopoiesis and adaptive immunity. Cell Rep. *17*, 3178–3192.

Matsuoka, S., Tsuji, K., Hisakawa, H., Xu, M., Ebihara, Y., Ishii, T., Sugiyama, D., Manabe, A., Tanaka, R., Ikeda, Y., et al. (2001). Generation of definitive hematopoietic stem cells from murine early yolk sac and paraaortic splanchnopleures by aorta-gonad-mesonephros region-derived stromal cells. Blood *98*, 6–12.

Moins-Teisserenc, H., Busson, M., Herda, A., Apete, S., Peffault de Latour, R., Robin, M., Xhaard, A., Toubert, A., and Socie, G. (2013). CD19(+)CD5(+) B cells and B1-like cells following allogeneic hematopoietic stem cell transplantation. Biol. Blood Marrow Transpl. *19*, 988–991.

Moro, K., Yamada, T., Tanabe, M., Takeuchi, T., Ikawa, T., Kawamoto, H., Furusawa, J., Ohtani, M., Fujii, H., and Koyasu, S. (2010). Innate production of T(H)2 cytokines by adipose tissue-associated c-Kit(+)Sca-1(+) lymphoid cells. Nature *463*, 540–544.

Nakano, T., Kodama, H., and Honjo, T. (1994). Generation of lymphohematopoietic cells from embryonic stem cells in culture. Science *265*, 1098–1101.

Nishikawa, S.I., Nishikawa, S., Kawamoto, H., Yoshida, H., Kizumoto, M., Kataoka, H., and Katsura, Y. (1998). In vitro generation of lymphohematopoietic cells from endothelial cells purified from murine embryos. Immunity *8*, 761–769.

Pearson, S., Cuvertino, S., Fleury, M., Lacaud, G., and Kouskoff, V. (2015). In vivo repopulating activity emerges at the onset of hematopoietic specification during embryonic stem cell differentiation. Stem Cell Reports *4*, 431–444.

Potocnik, A.J., Nerz, G., Kohler, H., and Eichmann, K. (1997). Reconstitution of B cell subsets in Rag deficient mice by transplantation of in vitro differentiated embryonic stem cells. Immunol. Lett. *57*, 131–137.

Robinson, M.D., McCarthy, D.J., and Smyth, G.K. (2010). edgeR: a Bioconductor package for differential expression analysis of digital gene expression data. Bioinformatics *26*, 139–140.

Schmitt, T.M., de Pooter, R.F., Gronski, M.A., Cho, S.K., Ohashi, P.S., and Zuniga-Pflucker, J.C. (2004). Induction of T cell development and establishment of T cell competence from embryonic stem cells differentiated in vitro. Nat. Immunol. *5*, 410–417.

Schulz, C., Gomez Perdiguero, E., Chorro, L., Szabo-Rogers, H., Cagnard, N., Kierdorf, K., Prinz, M., Wu, B., Jacobsen, S.E., Pollard, J.W., et al. (2012). A lineage of myeloid cells independent of Myb and hematopoietic stem cells. Science *336*, 86–90.

Sugimura, R., Jha, D.K., Han, A., Soria-Valles, C., da Rocha, E.L., Lu, Y.F., Goettel, J.A., Serrao, E., Rowe, R.G., Malleshaiah, M., et al. (2017). Haematopoietic stem and progenitor cells from human pluripotent stem cells. Nature *545*, 432–438.

Suzuki, N., Yamazaki, S., Yamaguchi, T., Okabe, M., Masaki, H., Takaki, S., Otsu, M., and Nakauchi, H. (2013). Generation of engraftable hematopoietic stem cells from induced pluripotent stem cells by way of teratoma formation. Mol. Ther. *21*, 1424–1431.

Tian, Y., Xu, J., Feng, S., He, S., Zhao, S., Zhu, L., Jin, W., Dai, Y., Luo, L., Qu, J.Y., et al. (2017). The first wave of T lymphopoiesis in zebrafish arises from aorta endothelium independent of hematopoietic stem cells. J. Exp. Med. *214*, 3347–3360.

Tsukada, M., Ota, Y., Wilkinson, A.C., Becker, H.J., Osato, M., Nakauchi, H., and Yamazaki, S. (2017). In vivo generation of engraftable murine hematopoietic stem cells by Gfi1b, c-Fos, and Gata2 overexpression within teratoma. Stem Cell Reports *9*, 1024–1033.

Wang, Y., Yates, F., Naveiras, O., Ernst, P., and Daley, G.Q. (2005). Embryonic stem cell-derived hematopoietic stem cells. Proc. Natl. Acad. Sci. U S A *102*, 19081–19086.

Yoshimoto, M. (2015). The first wave of B lymphopoiesis develops independently of stem cells in the murine embryo. Ann. N. Y. Acad. Sci. *1362*, 16–22.

Yoshimoto, M., Heike, T., Chang, H., Kanatsu-Shinohara, M., Baba, S., Varnau, J.T., Shinohara, T., Yoder, M.C., and Nakahata, T. (2009). Bone marrow engraftment but limited expansion of hematopoietic cells from multipotent germline stem cells derived from neonatal mouse testis. Exp. Hematol. *37*, 1400–1410.

Yoshimoto, M., Montecino-Rodriguez, E., Ferkowicz, M.J., Porayette, P., Shelley, W.C., Conway, S.J., Dorshkind, K., and Yoder, M.C. (2011). Embryonic day 9 yolk sac and intra-embryonic hemogenic endothelium independently generate a B-1 and marginal zone progenitor lacking B-2 potential. Proc. Natl. Acad. Sci. U S A *108*, 1468–1473.

Yoshimoto, M., Porayette, P., Glosson, N.L., Conway, S.J., Carlesso, N., Cardoso, A.A., Kaplan, M.H., and Yoder, M.C. (2012). Autonomous murine T-cell progenitor production in the extra-embryonic yolk sac before HSC emergence. Blood *119*, 5706–5714.